Frequency-Shaped Optimal Control of Unbalance Response in Active Magnetic Bearing System

Chong-Won Lee
Center for Noise and Vibration Control, Department of Mechanical Engineering, KAIST
Science Town, Taejon, 305-701, Korea
Tel +82-42-869-3016, Fax +82-42-869-8220, E-mail: cwlee@hanbit.kaist.ac.kr

Young-Ho Ha
R & D 2 Department, Technical Center, Daewoo Precision Industries Ltd.
Kumjeong P.O. Box 25, Pusan, 609-600, Korea
Tel +82-51-509-2298, Fax +82-51-508-3340

Abstract: Optimal control with frequency-shaped cost functional is applied to the control of unbalance response in active magnetic bearing system. The active magnetic bearing system is modeled as a symmetric rigid rotor supported by two anisotropic bearings. The cost functional is expressed in terms of frequency dependent weighting matrices defined in the frequency domain so that a penalty is given over the rotational speed of rotor. The control scheme consists of two closed loops: one for the stabilization of system and another for the control of unbalance response. The control method renders the varying optimal feedback gains, as the rotational speed changes.

The performance of this control method is evaluated through simulations to check its applicability to suppression of unbalance response or force in active magnetic bearing system. Simulation work is carried out at three rotational speeds: below the first critical speed, between the first and second critical speeds, and above the second critical speed. It is robust in the sense that it does not require accurate estimation of unbalance, whereas it still guarantees the system stability.

1 Introduction

Mass imbalance of the rotor in active magnetic bearing(AMB) system causes the alternating bearing forces and synchronous shaft whirl motions [1]. The alternating bearing forces can be alleviated by adding band-reject filter circuits in feedback loops or generating a rotating magnetic force. This would block the synchronous vibration from feedback and make AMB soft at the rotational speed. Thus the rotor tends to rotate with respect to its mass center reducing the unbalance force exerted to the bearing [2, 3]. The synchronous whirl motions of the shaft can be suppressed by providing electromagnetic forces which counteract the synchronous response arising from the unbalance [3, 4].

In this work, the synchronous motion of AMB system is controlled by optimal control with frequency-shaped cost functional. The cost functional is expressed in terms of frequency dependent weighting matrices defined in the frequency domain so that a penalty is given over a specific range of frequency [5, 6]. This frequency domain optimal control problem can be expressed as a time domain linear quadratic state optimal control problem via Parseval's theorem. We can effectively control the unbalance response of AMB system because this method renders the varying feedback gains according to rotational speed change of AMB system.

2 Optimal Unbalance Control in AMB with Frequency- Shaped Cost Functional

2.1 Equations of motion of rigid rotor AMB system

Consider a rigid rotor magnetic bearing system, which can be modeled as a symmetric rigid rotor supported by two anisotropic bearings, as shown in Figure 1. Then the equation of motion can be expressed, in the bearing coordinate, as

$$\mathbf{M}\ddot{\mathbf{q}}(t) + \mathbf{G}\dot{\mathbf{q}}(t) = \mathbf{f}_t(t) \tag{1}$$

where

$$\mathbf{q}(t) = \{y_1(t)\ y_2(t)\ z_1(t)\ z_2(t)\}^{\mathrm{T}},$$

$$\mathbf{f}_t = \mathbf{f}_m(t) + \mathbf{f}_e(t) = \{f_{y1}(t)\ f_{y2}(t)\ f_{z1}(t)\ f_{z2}(t)\}^{\mathrm{T}},$$

$$\mathbf{f}_e(t) = \{f_{ey1}(t)\ f_{ey2}(t)\ f_{ez1}(t)\ f_{ez2}(t)\}^{\mathrm{T}},$$

$$\mathbf{M} = \begin{bmatrix} ml_2^2 + j_d & ml_1l_2 - j_d & 0 & 0 \\ ml_1l_2 - j_d & ml_1^2 + j_d & 0 & 0 \\ 0 & 0 & ml_2^2 + j_d & ml_1l_2 - j_d \\ 0 & 0 & ml_1l_2 - j_d & ml_1^2 + j_d \end{bmatrix},$$

$$\mathbf{G} = \begin{bmatrix} 0 & 0 & j_p & -j_p \\ 0 & 0 & -j_p & j_p \\ -j_p & j_p & 0 & 0 \\ j_p & -j_p & 0 & 0 \end{bmatrix}\Omega,$$

$$j_d = J_d/b_t^2,\ j_p = J_p/b_t^2,\ l_1 = b_1/b_t,\ l_2 = b_2/b_t,\ b_t = b_1 + b_2,$$

where $\mathbf{M}$ and $\mathbf{G}$ are the mass and gyroscopic matrices, respectively; $\mathbf{q}(t)$, $\mathbf{f_m}(t)$ and $\mathbf{f_e}(t)$ are the displacement, magnetic and external force vectors defined in the bearing coordinate; m, J_p and J_d are the mass, polar and diametrical mass moments of inertia of the rotor respectively; Ω is the rotational speed of the rotor; b_1 and b_2 are the distances of the two radial magnetic bearings from the mass center of the rotor. The subscript T denotes the transpose of vectors.

Linearizing the magnetic force with respect to the neutral position [7, 8], the magnetic force vector $\mathbf{f_m}(t)$ due to small perturbations, $\mathbf{q}(t)$, in air gap, and, $\mathbf{i}(t)$, in current, can be expressed as

$$\mathbf{f_m}(t) = \mathbf{K_i}\mathbf{i}(t) - \mathbf{K_q}\mathbf{q}(t) \tag{2}$$

$$\mathbf{K_i} = diag\begin{bmatrix} K_{i_{y1}} & K_{i_{y2}} & K_{i_{z1}} & K_{i_{z2}} \end{bmatrix},$$

$$\mathbf{K_q} = diag\begin{bmatrix} K_{y1} & K_{y2} & K_{z1} & K_{z2} \end{bmatrix},$$

$$\mathbf{i}(t) = \begin{Bmatrix} i_{y1}(t) & i_{y2}(t) & i_{z1}(t) & i_{z2}(t) \end{Bmatrix}^{\mathrm{T}},$$

Here K_q and K_{iq} are the negative position stiffness and the current stiffness of each magnet, respectively.

By combining equations (1) and (2), we obtain

$$\mathbf{M}\ddot{\mathbf{q}}(t) + \mathbf{G}\dot{\mathbf{q}}(t) + \mathbf{K_q}\mathbf{q}(t) = \mathbf{f_i}(t) + \mathbf{f_e}(t), \tag{3}$$

where $\mathbf{f_i}(t) = \mathbf{K_i}\mathbf{i}(t)$.

When the rotor with eccentricity of ε rotates around the inertial axis with an inclination angle of ϕ, equation (3) can be rewritten in the state space form as

$$\dot{\mathbf{x}}(t) = \mathbf{A}\mathbf{x}(t) + \mathbf{B}\mathbf{u}(t) + \mathbf{D_o}\mathbf{f_e}(t), \tag{4-a}$$

where

$$\mathbf{q}(t) = \mathbf{C}\mathbf{x}(t) \tag{4-b}$$

where

$$\mathbf{A} = \begin{bmatrix} \mathbf{0}_4 & \mathbf{I}_4 \\ \mathbf{M}^{-1}\mathbf{K_q} & -\mathbf{M}^{-1}\mathbf{G} \end{bmatrix}, \quad \mathbf{B} = \begin{bmatrix} \mathbf{0}_4 \\ \mathbf{M}^{-1}\mathbf{K_i} \end{bmatrix}, \quad \mathbf{D_o} = \begin{bmatrix} \mathbf{0}_4 \\ \mathbf{D_1} \end{bmatrix},$$

$$\mathbf{x}(t) = \begin{Bmatrix} \mathbf{q}(t) \\ \dot{\mathbf{q}}(t) \end{Bmatrix}, \quad \mathbf{u}(t) = \begin{Bmatrix} i_{y1}(t) & i_{y2}(t) & i_{z1}(t) & i_{z2}(t) \end{Bmatrix}^{\mathrm{T}},$$

$$\mathbf{C} = \begin{bmatrix} \mathbf{I}_4 & \mathbf{0}_4 \end{bmatrix}, \quad \mathbf{D_1} = \mathbf{M}^{-1}\begin{bmatrix} l_2 & 0 & -1 & 0 \\ l_1 & 0 & 1 & 0 \\ 0 & l_2 & 0 & 1 \\ 0 & l_1 & 0 & -1 \end{bmatrix},$$

$$\mathbf{f_e} = diag\begin{bmatrix} \Phi_o\cos(\Omega t + \delta_o) & \Phi_o\sin(\Omega t + \delta_o) & \Psi_o\sin(\Omega t + \gamma_o) & \Psi_o\cos(\Omega t + \gamma_o) \end{bmatrix}$$

$$\Phi_o = m\varepsilon\Omega^2, \quad \Psi_o = (J_d - J_p)\phi\Omega^2 / b_t \ .$$

where $\mathbf{I_4}$ and $\mathbf{0_4}$ are the 4 × 4 identity and null matrices, respectively, and δ_o and γ_o are the phases associated with the static and dynamic unbalances, respectively.

2.2 Controller design of rigid rotor AMB system

Consider the system (4) and the associated performance index

$$J(\mathbf{u}) = \int_{t_o}^{\infty}[\mathbf{x}^{\mathrm{T}}(t)\,\mathbf{Q_x}\,\mathbf{x}(t) + \mathbf{u}^{\mathrm{T}}(t)\,\mathbf{R}\,\mathbf{u}(t)]dt \tag{5}$$

where $\mathbf{Q_x}$ and $\mathbf{R}$ are the constant positive semi-definite and positive definite matrices, respectively, and $\mathbf{x}(t_o)$ is given. The performance index (5) may be rewritten in the frequency domain using Parseval's theorem [9] as

$$J(\mathbf{U}) = \frac{1}{2\pi}\int_{-\infty}^{\infty}[\overline{\mathbf{X}}^{\mathrm{T}}(\mathrm{j}\omega)\,\mathbf{Q_x}\,\mathbf{X}(\mathrm{j}\omega) + \overline{\mathbf{U}}^{\mathrm{T}}(\mathrm{j}\omega)\,\mathbf{R}\,\mathbf{U}(\mathrm{j}\omega)]d\omega \ , \tag{6}$$

where "$-$" implies the complex conjugate, and $\mathbf{X}(\mathrm{j}\omega)$ and $\mathbf{U}(\mathrm{j}\omega)$ are the Fourier transforms of $\mathbf{x}(t)$ and $\mathbf{u}(t)$, respectively. To further penalize the unbalance response, we can modify the above performance index, by using a frequency shaping technique, as follows: Consider a band pass filter defined as

$$V_q(\mathrm{j}\omega) = N(\mathrm{j}\omega)Q(\mathrm{j}\omega), \ N(\mathrm{j}\omega) = \frac{\mathrm{j}\alpha_o\omega}{-\omega^2 + 2\mathrm{j}\zeta\Omega\omega + \Omega^2}, \tag{7}$$

where $v_q(t)$, $q = y_1, \ y_2, \ z_1, \ z_2$, is the filtered output of $q(t)$, and , $V_q(\mathrm{j}\omega)$ and $Q(\mathrm{j}\omega)$ are the Fourier transforms of $v_q(t)$ and $q(t)$, respectively. Here ζ and α_o are the damping ratio and input gain of the band pass filter, respectively. Note here that the center frequency is tuned to the rotational speed. Equation (7) is equivalent to the differential equation given by

$$\frac{d^2v_q(t)}{dt^2} + 2\zeta\Omega\frac{dv_q(t)}{dt} + \Omega^2 v_q(t) = \alpha_o\dot{q}(t). \tag{8}$$

Rewriting equation (8) in the state space form, we get

$$\dot{\mathbf{v}}_{\mathbf{q}}(t) = \mathbf{A_v}\mathbf{v_q}(t) + \mathbf{B_v}\mathbf{w}(t), \tag{9}$$

where

$$\mathbf{A_v} = \begin{bmatrix} 0 & 1 \\ -\Omega^2 & -2\zeta\Omega \end{bmatrix}, \ \mathbf{B_v} = \begin{bmatrix} 0 & 0 \\ 0 & \alpha_o \end{bmatrix},$$

$$\mathbf{v_q}(t) = \begin{Bmatrix} v_q(t) \\ \dot{v}_q(t) \end{Bmatrix}, \quad \mathbf{w}(t) = \begin{Bmatrix} q(t) \\ \dot{q}(t) \end{Bmatrix} \ .$$

Then we can write the augmented plant state equation as

$$\dot{\mathbf{x}}_{\mathbf{e}}(t) = \mathbf{A_e}\mathbf{x_e}(t) + \mathbf{B_e}\mathbf{u}(t) + \mathbf{D_e}\mathbf{f_e}(t), \tag{10}$$

where

$$\mathbf{x_e}(t) = \begin{Bmatrix} \mathbf{v}(t) \\ \mathbf{x}(t) \end{Bmatrix}, \ \mathbf{A_e} = \begin{bmatrix} \mathbf{A_N} & \mathbf{A_{CN}} \\ \mathbf{0}_4 & \mathbf{A} \end{bmatrix}, \ \mathbf{B_e} = \begin{bmatrix} \mathbf{0}_4 \\ \mathbf{B} \end{bmatrix},$$

$$\mathbf{v}(t) = \begin{Bmatrix} v_{y_1}(t) & v_{y_2}(t) & v_{z_1}(t) & v_{z_2}(t) & \dot{v}_{y_1}(t) & \dot{v}_{y_2}(t) & \dot{v}_{z_1}(t) & \dot{v}_{z_2}(t) \end{Bmatrix}^{\mathrm{T}}$$

$$\mathbf{A_N} = \begin{bmatrix} \mathbf{0}_4 & \mathbf{I}_4 \\ -\Omega^2\mathbf{I}_4 & -2\zeta\Omega\,\mathbf{I}_4 \end{bmatrix}, \mathbf{A_{CN}} = \begin{bmatrix} \mathbf{0}_4 & \mathbf{0}_4 \\ \mathbf{0}_4 & \alpha_o\mathbf{I}_4 \end{bmatrix},$$

$$\mathbf{D}_e = \begin{bmatrix} \mathbf{0}_4 \\ \mathbf{0}_4 \\ \mathbf{D}_o \end{bmatrix}.$$

Note that the augmented plant states consist of the original and filtered ones. The state feedback control law for the augmented plant, $\mathbf{u}_f(t) = -\mathbf{K}_x\mathbf{x}(t) - \mathbf{K}_v\mathbf{v}(t)$, is equivalent to the dynamic state feedback law for the original plant as [10]

$$\mathbf{U}_f(j\omega) = -\mathbf{K}_f(j\omega)\mathbf{X}(j\omega), \quad (11.a)$$

$$\mathbf{K}_f(j\omega) = \mathbf{K}_x + \mathbf{K}_v(j\omega\mathbf{I} - \mathbf{A}_N)^{-1}\mathbf{A}_{CN}, \quad (11.b)$$

where $\mathbf{U}_f(j\omega)$ is the Fourier transform of $\mathbf{u}_f(t)$ and, $\mathbf{K}_x$ and $\mathbf{K}_v$ are the 4 × 8 feedback gain matrices.

Now, in order to further penalize the unbalance response, we modify the performance index (6) as

$$J(\mathbf{U}) = \frac{1}{2\pi}\int_{-\infty}^{\infty}[\overline{\mathbf{X}}^T(j\omega)\mathbf{Q}_e(j\omega)\mathbf{X}(j\omega) + \overline{\mathbf{U}}^T(j\omega)\mathbf{R}\,\mathbf{U}(j\omega)]d\omega$$

where (12)

$$\mathbf{Q}_e(j\omega) = \mathbf{Q}_x + \mathbf{A}_{CN}^T(j\omega\mathbf{I} - \mathbf{A}_N)^{-T}\mathbf{Q}_v(j\omega\mathbf{I} - \mathbf{A}_N)^{-1}\mathbf{A}_{CN}.$$

Here $\mathbf{Q}_v$ is the positive semi-definite matrix. It can then be easily proven that the cost functional (12) is equivalent to

$$J(\mathbf{u}) = \int_0^{\infty}[\mathbf{x}_e^T(t)\mathbf{Q}_e\,\mathbf{x}_e(t) + \mathbf{u}^T(t)\mathbf{R}\,\mathbf{u}(t)]\,dt, \quad (13)$$

where

$$\mathbf{Q}_e = \begin{bmatrix} \mathbf{Q}_{11} & \mathbf{Q}_{12} \\ \mathbf{Q}_{21} & \mathbf{Q}_{22} \end{bmatrix}, \quad \mathbf{Q}_x = \begin{bmatrix} \mathbf{q}_{11} & \mathbf{q}_{12} \\ \mathbf{q}_{21} & \mathbf{q}_{22} \end{bmatrix}, \quad \mathbf{Q}_{22} = \mathbf{q}_{22},$$

$$\mathbf{Q}_{11} = \begin{bmatrix} \beta_p^2\mathbf{I}_4 & \mathbf{0}_4 & \mathbf{0}_4 \\ \mathbf{0}_4 & \beta_d^2\mathbf{I}_4 & \mathbf{0}_4 \\ \mathbf{0}_4 & \mathbf{0}_4 & \mathbf{q}_{11} \end{bmatrix}, \quad \mathbf{Q}_{12} = \begin{bmatrix} \mathbf{0}_4 \\ \mathbf{0}_4 \\ \mathbf{q}_{12} \end{bmatrix},$$

$$\mathbf{Q}_{21} = \begin{bmatrix} \mathbf{0}_4 \\ \mathbf{0}_4 \\ \mathbf{q}_{21} \end{bmatrix}^T, \quad \mathbf{R} = \mathbf{I}_4$$

Here $\mathbf{q}_{11}$, $\mathbf{q}_{12}$, $\mathbf{q}_{21}$ and $\mathbf{q}_{22}$ are the partitioned 4 × 4 original weighting matrices and, β_π and β_d are the weighting factors. Then the control input, $\mathbf{u}_f(t)$, of the optimal controller with the frequency-shaped cost functional can be represented as

$$\mathbf{u}_f(t) = -\mathbf{K}_v\mathbf{v}(t) - \mathbf{K}_x\mathbf{x}(t) \quad (14)$$

Note that equation (14) reduces to the conventional optimal control scheme $\mathbf{u}_o(t) = -\mathbf{K}_x\mathbf{x}(t)$ when $\mathbf{K}_v\mathbf{v}(t) = \mathbf{0}$. Figure 2 shows the block diagram of the unbalance response control of AMB system by the optimal control with the frequency-shaped cost functional.

The Fourier transform of equation (4) gives

$$(j\omega\mathbf{I} - \mathbf{A})\mathbf{X}(j\omega) = \mathbf{B}\mathbf{U}(j\omega) + \mathbf{D}_o\mathbf{F}_e(j\omega) \quad (15.a)$$

$$\mathbf{Q}(j\omega) = \mathbf{C}\mathbf{X}(j\omega) \quad (15.b)$$

where $\mathbf{Q}(j\omega)$ and $\mathbf{F}_e(j\omega)$ are the Fourier transforms of $\mathbf{q}(t)$ and $\mathbf{f}_e(t)$, respectively, and $\mathbf{C}$ is the 4×8 output matrix.

By using equations (11) and (15), we can write the relation between $\mathbf{F}_e(j\omega)$ and $\mathbf{Q}(j\omega)$ in the optimal control with frequency-shaped cost functional as

$$\mathbf{Q}(j\omega) = \mathbf{C}\left[j\omega\mathbf{I} - \mathbf{A} + \mathbf{B}\left\{\mathbf{K}_x + \mathbf{K}_v(j\omega\mathbf{I} - \mathbf{A}_N)^{-1}\mathbf{A}_{CN}\right\}\right]^{-1}\mathbf{D}_o\mathbf{F}_e(j\omega).$$

The relation between, $\mathbf{V}_r(j\omega)$, the reference input, and, $\mathbf{Q}(j\omega)$, the displacement of the rotor, can then be written as

$$\mathbf{Q}(j\omega) = \mathbf{C}\left[j\omega\mathbf{I} - \mathbf{A} + \mathbf{B}H_A(j\omega)\left\{\mathbf{K}_x + \mathbf{K}_f(j\omega\mathbf{I} - \mathbf{A}_N)^{-1}\mathbf{A}_{CN}\right\}\right]^{-1} \bullet H_A(j\omega)\mathbf{D}_o\mathbf{K}_i\mathbf{V}_r(j\omega), \quad (16)$$

where $H_A(j\omega)$ represents the frequency response characteristics of the power amplifier unit.

3 Numerical Simulation

In this section, performance of the optimal control with frequency shaped cost functional is evaluated through simulations to check its applicability to suppression of unbalance response or reduction of unbalance force in AMB system.

The AMB system parameters for simulation are given as:

$$\mathbf{M} = \begin{bmatrix} 5.31 & -1.34 & 0 & 0 \\ -1.34 & 7.03 & 0 & 0 \\ 0 & 0 & 5.31 & -1.34 \\ 0 & 0 & -1.34 & 7.03 \end{bmatrix},$$

$$\mathbf{G} = 0.245\begin{bmatrix} 0 & 0 & 1 & -1 \\ 0 & 0 & -1 & 1 \\ -1 & 1 & 0 & 0 \\ 1 & -1 & 0 & 0 \end{bmatrix}\Omega,$$

$$\mathbf{K}_q = diag[1.11 \quad 1.15 \quad 1.11 \quad 1.15] \times 10^6,$$

$$\mathbf{K}_i = diag[256 \quad 260 \quad 256 \quad 260],$$

$$\varepsilon = 5\mu m,\ \phi = 0.018,\ \delta_o = 0,\ \gamma_o = 0.78.$$

The parameters required for the controller design are empirically determined as:

$$\beta_p^2 = 5\times10^8,\quad \beta_d^2 = 5\times10^3,\quad \mathbf{q}_{11} = 5\times10^6\times\mathbf{I}_4,$$

$$\mathbf{q}_{12} = 0.5\times\mathbf{I}_4,\quad \mathbf{q}_{21} = \mathbf{q}_{12}^T,\quad \mathbf{Q}_{22} = 10\times\mathbf{I}_4,\quad \zeta = 0.02.$$

Then the feedback gain matrices for a sub-critical speed Ω = 3,000 rpm and $\alpha_o = 10$ are calculated to be

$$\mathbf{K}_x = \begin{bmatrix} 9199 & 1.2 & 121 & -114 & 10 & -1.2 & 0 & 0 \\ 4 & 9356 & -112 & 105 & -1.2 & 11.5 & 0 & 0 \\ -121 & 114 & 9199 & 1.2 & 0 & 0 & 10 & -1.2 \\ 112 & -105 & 4 & 9356 & 0 & 0 & -1.2 & 11.5 \end{bmatrix},$$

$$\mathbf{K_v} = \begin{bmatrix} \underline{7857} & 1673 & 49 & -19 & 24 & 0.5 & 0.5 & -0.4 \\ 1691 & \underline{5904} & -17 & -6.54 & -0.4 & 25 & -0.4 & 0.4 \\ -49 & 19 & \underline{7857} & 1673 & -0.5 & 0.4 & 24 & -0.5 \\ 17 & 6.5 & 1691 & \underline{5904} & 0.4 & -0.4 & -0.4 & 25 \end{bmatrix}.$$

Note here that the underlined elements in $\mathbf{K_v}$, which are significantly larger than the neighboring elements, are all positive. It implies that, when the rotor is run below the first critical speed, the bearing stiffness and thus the natural frequencies of the closed-loop AMB system are further increased by the optimal control with frequency-shaped cost functional. For example, the first critical speed is increased from 3,860 rpm to 4,340 rpm. Figure 3(a) shows the typical closed loop transfer function, possessing the characteristics of a notch filter but still ensuring the stability of the system. Figure 4(a) is the corresponding unbalance response plot against the rotational speed, implying that, when the rotor operates close to the tuned center frequency, the proposed method remains superior to the conventional method in attenuation of unbalance responses.

When Ω = 7,800 rpm and α_o=35, the feedback gain matrices are calculated to be

$$\mathbf{K_x} = \begin{bmatrix} 9182 & 20 & 328 & -307 & 10 & -1 & 0 & 0 \\ 186 & 9341 & -302.6 & 285 & -1 & 11 & 0 & 0 \\ -328 & 307 & 9182 & 20 & 0 & 0 & 10 & -1 \\ 303 & -285 & 186 & 9341 & 0 & 0 & -1 & 11 \end{bmatrix},$$

$$\mathbf{K_v} = \begin{bmatrix} \underline{-7597} & 347 & -382 & 327 & 9.8 & 1.4 & 0 & 0 \\ 342 & \underline{-8257} & 333 & -282 & 1.4 & 8.2 & 0 & 0 \\ 382 & -327 & \underline{-7597} & 347 & 0 & 0 & 9.8 & 1.4 \\ -333 & 282 & 342 & \underline{-8257} & 0 & 0 & 1.4 & 8.2 \end{bmatrix}$$

Note that the underlined elements in $\mathbf{K_v}$ are all negative. It means that the proposed method tends to further lower the natural frequencies of the conventional optimal controlled system, when the rotor is run beyond the second critical speed. For example, the second critical speed is decreased from 5,020 rpm to 4,290 rpm. Figure 4(b) is the corresponding unbalance response plot against the rotational speed and Figure 3(b) shows the typical closed loop transfer function. Note that the high value of α_o is chosen as the operational speed increases, particularly above the critical speeds.

When Ω = 4,500 rpm and α_o = 15, the gain matrices are calculated to be

$$\mathbf{K_x} = \begin{bmatrix} 9196 & 4.3 & 179 & -168 & 10 & -1.2 & 0 & 0 \\ 7.2 & 9353 & -166 & 157 & -1.2 & 12 & 0 & 0 \\ -179 & 168 & 9196 & 4.3 & 0 & 0 & 10 & -1.2 \\ 166 & -157 & 7.2 & 9353 & 0 & 0 & -1.2 & 12 \end{bmatrix}$$

$$\mathbf{K_v} = \begin{bmatrix} \underline{3123} & \underline{3196} & -156 & 187 & 31.2 & 0.9 & 0.6 & -0.5 \\ \underline{3213} & \underline{-544} & 194 & -213 & 1 & 30 & -0.5 & 0.4 \\ 156 & -187 & \underline{3123} & \underline{3196} & -0.6 & 0.5 & 31.2 & 0.9 \\ -194 & 213 & \underline{3213} & \underline{-544} & 05 & -0.4 & 1 & 30 \end{bmatrix}$$

Note that the underlined elements in $\mathbf{K_v}$, which are again significantly larger than the neighboring elements, can now be positive or negative. It implies that, when the rotor is run between the first and second critical speeds, the natural frequencies associated with the first(second) mode of the closed-loop AMB system are further decreased (increased) by the optimal control with frequency-shaped cost functional. The typical closed loop transfer function of closed loop is shown in Figure 3(c).

Table 1 compares the unbalance responses and the control inputs of the rigid rotor AMB system by the conventional optimal control and the proposed optimal control with frequency-shaped cost functional for Ω = 3,000, 4,000 and 7,800 rpm: the unbalance responses for the latter case are kept far less by a factor of 2 or more than for the former case, without increasing the control forces.

4 Conclusion

The optimal control with frequency-shaped cost functional applied to the unbalance response control of AMB system gives proper feedback gains, depending upon the rotational speed of the system: it gives high feedback gains at low rotational speed and low feedback gains at high rotational speed. In addition, this control method does not require accurate estimation of unbalance while it does not degrade the system stability. The proposed method is proved to be effective through numerical simulations.

Reference

1. T. Mizuno and T. Higuchi, "Design of Magnetic Bearing Controllers Based in Disturbance Estimation," Proc. of Second International Symposium on Magnetic Bearings, Tokyo, pp. 281-288, 1990
2. H. M. Chen and M. S. Darlow, "Magnetic Bearing with Rotating Force Control," Trans. of ASME, Journal of Tribology, Vol. 110, pp. 100-105, 1988
3. T. Higuchi, M. Otsuka, T. Mizuno and T. Ide, "Application of Periodic Learning Control with Inverse Transfer Function Compensation in Totally Active Magnetic Bearings," Proc. of Second International Symposium on Magnetic Bearings, Tokyo, pp. 257-264, 1990
4. A. Sinha, K. L. Mease and K. W. Wang, "Sliding Mode Control of a Rigid Rotor Via Magnetic Bearings," ASME Conference, Modal Analysis, Modeling, Diagnosis, and Control - Analytical and Experimental, DE-Vol. 38, pp. 209-217, 1991
5. N. K. Gupta, "Frequency-Shaped Cost Functionals: Extension of Linear-Quadratic-Gaussian Design Methods," Journal of Guidance and Control, Vol. 3, No. 6, pp. 529-535, 1980
6. B. D. O. Anderson and J. B. Moore, *OPTIMAL CONTROL Linear Quadratic Methods*, Prentice-Hall, Inc. London, 1990
7. C. W. Lee and J .S. Kim "Modal Testing and Suboptimal Vibration control of Flexible Rotor Bearing System by Using a Magnetic Bearing," Trans. of ASME,

Journal of Dynamic Systems, Measurement, and Control, Vol. 114, pp. 244-252, 1992

8. C. W. Lee, Y. H. Ha, C. Y. Joh and C. S. Kim, "Identification of Active Magnetic Bearing System Using Directional Frequency Response Functions," Trans. of ASME, Journal of Dynamic Systems, Measurement, and Control, (Accepted), 1996
9. I. Stakgold, *Boundary Value Problems of Mathematical Physics, Volume I,* The MACMILLAN Company, London, 1972

Table 1 Comparison of the unbalance responses and the control inputs of the AMB system.

Conventional Method / Proposed Method						
Rotational Speed	3,000 rpm		4,500 rpm		7,800 rpm	
Bearing No.	#1	#2	#1	#2	#1	#2
Whirl Radius, μm	11.7 / 4.7	15.8 / 6.5	20.6 / 6.4	25.5 / 8.5	17.8 / 8.8	19.5 / 11.1
Max. Control Input, N	30 / 24	40 / 33	52 / 40	73 / 53	55 / 40	67 / 51

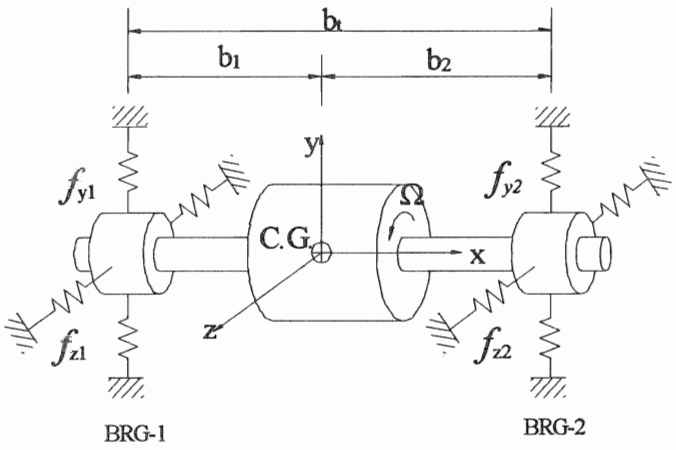

Figure 1 Modeling of a rigid rotor supported by two anisotropic magnetic bearings.

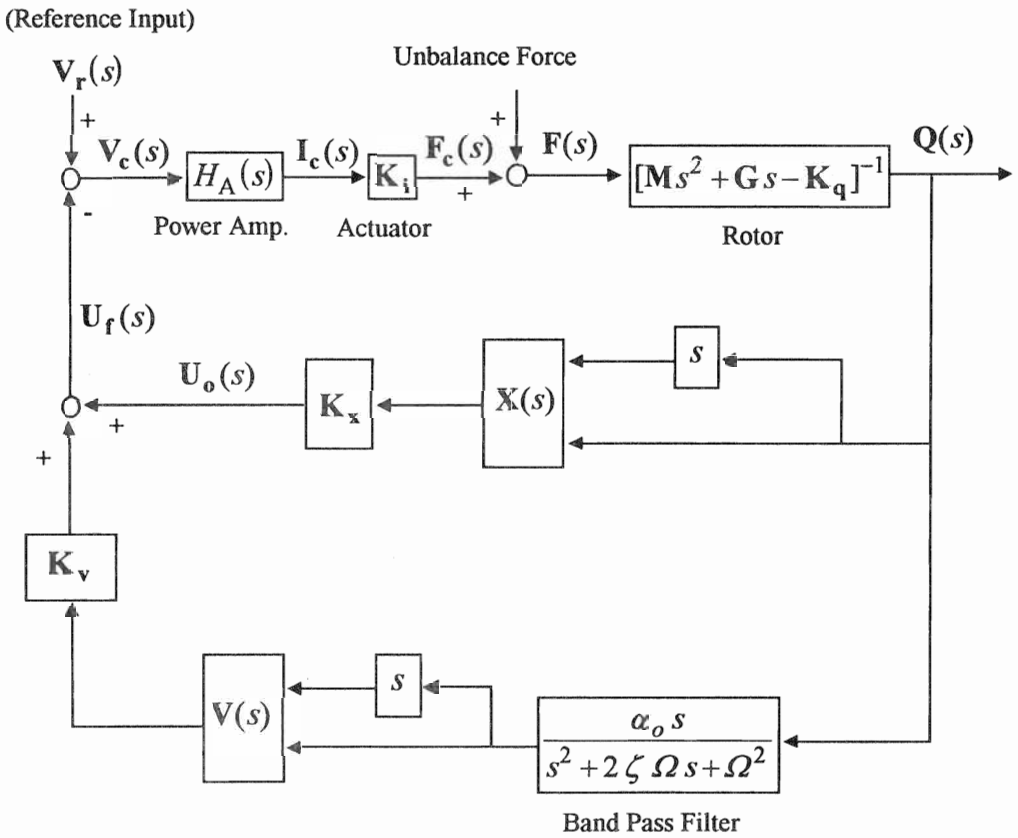

Figure 2 Block diagram of AMB system by optimal control with frequency-shaped cost functional

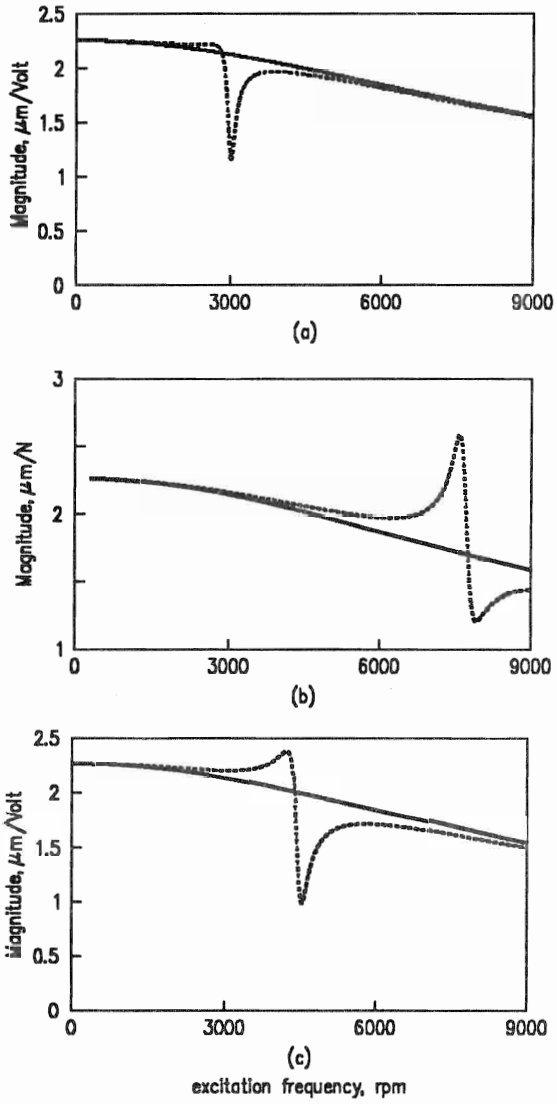

Figure 3 Transfer function between V_{h_1} and y_1 for the center frequency of (a) 3,000 rpm (b)7,800 rpm (c) 4,500rpm : ——— conventional; ·------· proposed.

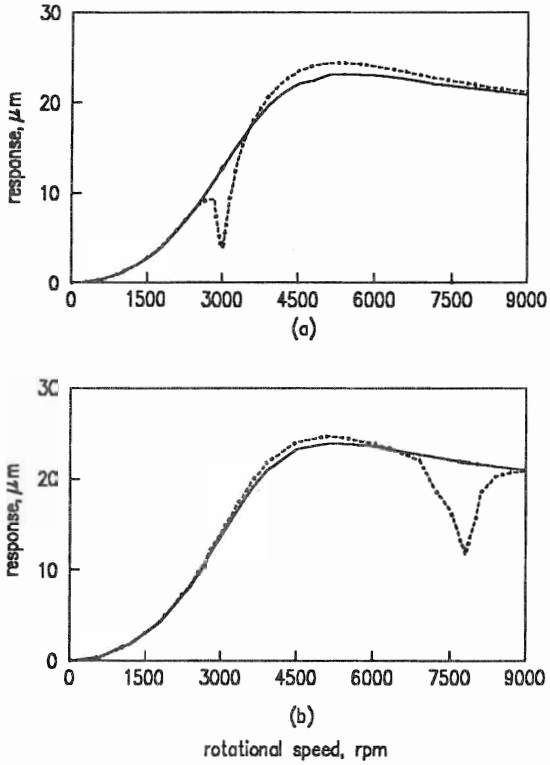

Figure 4 Unbalance response for the center frequency tuned to (a) 3,000 rpm and (b) 7,800 rpm : ——— conventional ·------· proposed